

Quasiparticle electronic structure of bismuth telluride in the GW approximationEmmanouil Kioupakis,^{1,2,3} Murilo L. Tiago,^{1,2,4} and Steven G. Louie^{1,2}¹*Department of Physics, University of California, Berkeley, California 94720, USA*²*Materials Sciences Division, Lawrence Berkeley National Laboratory, Berkeley, California 94720, USA*³*Materials Department, University of California, Santa Barbara, California 93106, USA*⁴*Materials Science and Technology Division, Oak Ridge National Laboratory, Oak Ridge, Tennessee 37831, USA*

(Received 13 September 2010; published 9 December 2010)

The quasiparticle band structure of bismuth telluride (Bi_2Te_3), an important thermoelectric material that exhibits topologically insulating surface states, is calculated from first principles in the GW approximation. The quasiparticle energies are evaluated in fine detail in the first Brillouin zone using a Wannier-function interpolation method, allowing the accurate determination of the location of the band extrema (which is in the mirror plane) as well as the values of the quasiparticle band gap (0.17 eV) and effective-mass tensors. Spin-orbit interaction effects were included. The valence band exhibits two distinct maxima in the mirror plane that differ by just 1 meV, giving rise to one direct and one indirect band gap of very similar magnitude. The effective-mass tensors are in reasonable agreement with experiment. The Wannier interpolation coefficients can be used for the tight-binding parametrization of the band structure. Our work elucidates the electronic structure of Bi_2Te_3 and sheds light on its exceptional thermoelectric and topologically insulating properties.

DOI: [10.1103/PhysRevB.82.245203](https://doi.org/10.1103/PhysRevB.82.245203)

PACS number(s): 71.20.Nr, 71.18.+y, 72.15.Jf

I. INTRODUCTION

In addition to microelectronics and optoelectronics, semiconducting materials have applications in the fields of thermoelectric cooling and power generation.¹ Narrow gap semiconductors with a high electrical conductivity and Seebeck coefficient and a low thermal conductivity are good candidates for thermoelectric applications. The quality of a thermoelectric material is quantified by the dimensionless figure of merit $ZT = S^2 \sigma T / (\kappa_L + \kappa_e)$, where T is the absolute temperature, S is the Seebeck coefficient, σ the electrical conductivity, and κ_L and κ_e are the lattice and electronic thermal conductivities, respectively. Bismuth telluride (Bi_2Te_3) and its alloys with Sb and Se are the bulk materials with the highest known figure of merit at room temperature. Current research is focused on materials with nanoscale dimensions, such as thin films, quantum-dot superlattices, and nanowires, where manipulation of quantum confinement effects can further enhance thermoelectricity.² Recently, Bi_2Te_3 has also been shown to be a topological insulator^{3,4} with a single nondegenerate surface-state band exhibiting a Dirac cone structure.

To obtain an accurate electronic structure and the band gap of Bi_2Te_3 , the inclusion of self-energy corrections to the quasiparticle energies is needed. Density-functional theory (DFT) calculations in the local-density approximation (LDA) for the exchange-correlation potential^{5,6} can describe accurately the ground-state properties, such as the total energy and the bond lengths, for a large array of systems, but are inappropriate for excited-state properties, such as the quasiparticle energies and band gap. One way to amend this deficiency is to calculate the quasiparticle properties with appropriate many-electron effects included within the GW approximation.^{7,8} In the GW approach, the electron self-energy operator Σ is approximated by the first term in its diagrammatic expansion in terms of the dressed Green's function G and the screened Coulomb interaction W (Σ

$\approx iGW$). The quasiparticle eigenvalues are calculated within first-order perturbation theory, starting from a DFT calculation as the mean-field solution. The GW method has been applied to a variety of materials, ranging from narrow-gap semiconductors (such as InSb) to wide-band-gap insulators (such as LiF), and has produced excellent results.^{8–10}

Despite its importance, the quasiparticle band structure of Bi_2Te_3 has not yet been determined and constitutes a challenging computational task. First, the experimental band gap is small, on the order of 0.1 eV, therefore, a highly accurate first-principles method is needed. Moreover, the material is composed of heavier elements for which relativistic effects are important and the spin-orbit coupling interaction has a significant effect on the band structure: the inclusion of spin-orbit effects reduces the LDA gap by about 50% and shifts the position of the band extrema away from the Γ point to lower symmetry positions on the mirror plane of the first Brillouin zone (BZ), as reported in previous calculations^{11–15} and measured in experiment.^{16,17} Finally, to locate the exact position of the band extrema in \mathbf{k} space, one needs to calculate the energy eigenvalues for a large, refined set of \mathbf{k} points. This is feasible within standard DFT method but becomes substantially more demanding computationally upon inclusion of quasiparticle effects. In order to obtain the GW band structure for arbitrary \mathbf{k} points, we calculated the GW and spin-orbit coupling corrections¹⁸ on a coarse grid in the first BZ and made use of the Wannier interpolation formalism^{19–21} to interpolate the quasiparticle eigenvalues and spin-orbit perturbation matrix to any \mathbf{k} .

II. METHODOLOGY

We performed DFT/LDA calculations using the plane-wave *ab initio* pseudopotential method,²² employing Troullier-Martins²³ pseudopotentials and a 50 Ry plane-wave cut-off energy. The 4*f* and 5*d* states of Bi and the 4*d* states of Te were frozen into the pseudopotential core since they are

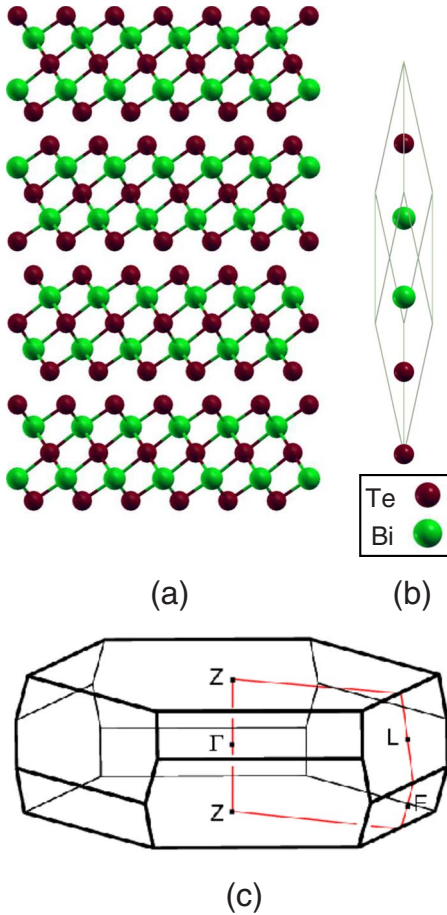


FIG. 1. (Color online) (a) Crystal structure of bismuth telluride as viewed from the direction parallel to the atomic planes. The planes consist of hexagonally arranged Bi or Te atoms. (b) The primitive unit cell of bismuth telluride used in the calculations with the five basis atoms designated. (c) The first Brillouin zone, where the mirror plane has been highlighted and special k -points denoted.

located at least 10 eV and 25 eV below the valence band minimum, respectively. Nonlinear core corrections were included.²⁴ Experimental lattice parameters²⁵ were used. The Brillouin zone was sampled using a $8 \times 8 \times 8$ Monkhorst-Pack grid²⁶ in the *ab initio* GW calculation. The static dielectric function was calculated with a 10 Ry plane-wave cutoff and a sum over 256 unoccupied bands, and extended to finite frequency using the generalized plasmon-pole model.⁸ Spin-orbit interaction effects were included within first-order perturbation theory by calculating the spin-orbit Hamiltonian matrix in the $L \cdot S$ approach¹⁸ using plane waves up to a cut-off energy of 20 Ry. For the maximally localized Wannier function generation process, we started with an initial guess of one s and three p orbitals per atom, the p orbitals facing along the nearest-neighbor direction, and used the disentanglement technique²⁰ to extract 20 Wannier functions out of 30 bands. The Wannier functions we obtained had a spread < 2.75 Å each. Our interpolation parameters provide an accurate and physically sound tight-binding parametrization of the band structure of Bi_2Te_3 .²⁷

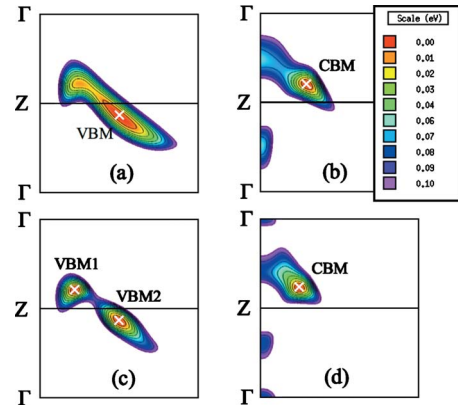


FIG. 2. (Color online) [(a) and (b)] Contour plots of the (a) highest valence and (b) lowest conduction energy bands of bismuth telluride in the high-symmetry mirror plane as calculated within DFT/LDA. The VBM and CBM have been denoted. [(c) and (d)] Contour plots of the GW quasiparticle (c) valence and (d) conduction bands. The valence band exhibits two distinct maxima in the mirror plane (VBM1 and VBM2) that differ by just 1 meV and are therefore indistinguishable within the current level of theory. The color scale indicates the energy difference from the corresponding band extremum, the isolines are spaced 10 meV apart and $Z = (0.5, 0.5, 0.5)$ in crystal coordinates.

III. RESULTS

Bi_2Te_3 has a layered structure consisting of slabs of five atomic planes, three hexagonal planes of tellurium atoms intercalated by two hexagonal planes of bismuth [Fig. 1(a)]. The system is periodic in the direction perpendicular to the slab plane with a periodicity of three slabs, i.e., the structure repeats itself every 15 atomic layers. While all bismuth atoms have six nearest tellurium neighbors, there are two kinds of tellurium sites, one (Te^1) with three bismuth and three tellurium (Te^1) nearest neighbors and another (Te^2) with six bismuth nearest neighbors. The five-layer slabs are made of atomic layers in the sequence Te^1 -Bi- Te^2 -Bi- Te^1 . The five-atom rhombohedral unit cell is shown in Fig. 1(b) and the first Brillouin zone in Fig. 1(c), where the special sixfold symmetric mirror plane is highlighted.

The conduction- and valence-band extrema lie on the sixfold symmetric mirror plane of the first BZ. Figures 2(a) and 2(b) show the contour plots of the (a) highest valence and (b) lowest conduction bands on this mirror plane as calculated in LDA. Spin-orbit coupling effects are included in this plot but GW corrections are not. Both bands have their extremum at a sixfold symmetric point, which means that upon n - or p -type doping, the material will exhibit six electron or hole Fermi-surface pockets, respectively. The position of the valence-band maximum (VBM) is at $k = (0.37, 0.54, 0.37)$ with a second local maximum at $(0.58, 0.67, 0.58)$ located just 11 meV lower in energy. The conduction-band minimum (CBM) is at $k = (0.58, 0.68, 0.58)$ with secondary local minima at Γ and along Γ - Z located at least 62 meV higher in energy. The band gap within LDA is indirect and has a value of 87 meV. However, LDA is known to underestimate the magnitude of band gaps⁸ and in this case it is found to be approximately 50% smaller than the experimental values of Table I.

TABLE I. The electronic band-gap magnitude and nature (direct/indirect) of bismuth telluride as calculated with various methods and measured by experiment.

| Method | D/I | E_g (eV) |
|---------------------------------------|-----|---------------|
| Experiment | | |
| Resistivity measurements ^a | | 0.171 |
| Optical measurements ^b | I | 0.150 |
| | D | 0.220 |
| Optical measurements ^c | I | 0.16 |
| Theory | | |
| This work, GW, VBM1 | D | 0.165 |
| This work, GW, VBM2 | I | 0.166 |
| This work, LDA | I | 0.087 |
| FLAPW, sX-LDA ^d | I | 0.154 |
| FLAPW, GGA ^e | D | 0.026 |
| FLAPW, H-L LDA ^f | I | 0.061 |
| FLAPW, GGA ^g | I | 0.13 |
| LMTO-ASA, LDA ^h | I | 0.11 |

^aReference 30.

^bReference 29.

^cReference 28.

^dReference 11.

^eReference 12, experimental lattice parameters.

^fReference 13.

^gReference 14.

^hReference 15.

 TABLE II. The effective-mass tensor parameters (α_{ij}) and extremum multiplicity (M) for the highest valence band of bismuth telluride as calculated with various methods and measured by experiment.

| Method | M | α_{xx} | α_{yy} | α_{zz} | α_{yz} | θ_{yz} (deg) |
|--------------------------------|-----|---------------|---------------|---------------|---------------|------------------------|
| Experiment | | | | | | |
| Shubnikov-de Haas ^a | 6 | 32.5 | 4.81 | 9.02 | 4.15 | 31.5 |
| Theory | | | | | | |
| This work, GW, VBM2 | 6 | 45.87 | 7.46 | 10.17 | 5.16 | 37.6 |
| This work, GW, VBM1 | 6 | 47.33 | 9.94 | 14.61 | -1.25 | -14.0 |
| This work, LDA | 6 | 56.93 | 4.84 | 6.64 | 5.21 | 40.1 |
| FLAPW, sX-LDA ^b | 6 | 39.5 | 3.8 | 5.2 | 6.2 | 41 |
| FLAPW, GGA ^c | 6 | 107.51 | 3.97 | 5.54 | 2.76 | 37.1 |
| FLAPW, GGA ^d | 6 | 30.6 | 10.6 | 13.8 | 1.1 | 17.4 |
| LMTO-ASA, LDA ^e | 6 | 109.3 | 5.2 | 6.2 | 3.1 | 35 |
| FLAPW, H-L LDA ^f | 6 | | | | | 42 |

^aReference 16.

^bReference 11.

^cReference 14.

^dReference 12, experimental lattice parameters.

^eReference 15.

^fReference 13.

 TABLE III. The effective-mass tensor parameters (α_{ij}) and extremum multiplicity (M) for the lowest conduction band of bismuth telluride as calculated with various methods and measured by experiment.

| Method | M | α_{xx} | α_{yy} | α_{zz} | α_{yz} | θ_{yz} (deg) |
|--------------------------------|-----|---------------|---------------|---------------|---------------|------------------------|
| Experiment | | | | | | |
| Shubnikov-de Haas ^a | 6 | 46.9 | 5.92 | 9.50 | 4.42 | 33.5 |
| Theory | | | | | | |
| This work, GW | 6 | 57.18 | 8.93 | 12.50 | 1.74 | 22.1 |
| This work, LDA | 6 | 82.25 | 7.96 | 10.39 | 3.72 | 36.0 |
| FLAPW, sX-LDA ^b | 6 | 52.2 | 8.0 | 7.3 | 3.8 | -42.4 |
| FLAPW, GGA ^c | 2 | 95.84 | 3.56 | 6.20 | 2.39 | 32.7 |
| FLAPW, GGA ^d | 6 | 34.7 | 3.9 | 13.3 | 2.8 | 15.5 |
| LMTO-ASA, LDA ^e | 2 | | | | | |
| FLAPW, H-L LDA ^f | 2 | | | | | 31 ^g |

^aReference 17.

^bReference 11.

^cReference 14.

^dReference 12, experimental lattice parameters.

^eReference 15.

^fReference 13.

^gAt second lowest conduction band edge.

The picture changes once GW corrections are included. GW increases the gap between the valence and conduction states to 0.17 eV and corrects the LDA underestimated result (Table I). The contour plots of the GW valence and conduction bands in the mirror plane are plotted in Figs. 2(c) and 2(d), respectively. The extrema of both bands are located away from the high-symmetry points and have a multiplicity of six. The valence band exhibits two distinct maxima that differ in energy by just 1 meV, labeled VBM1 and VBM2 in Fig. 2(c), located at (0.58,0.66,0.58) and (0.38,0.55,0.38), respectively. The conduction band has a unique minimum at $\mathbf{k}=(0.58,0.67,0.58)$. The local minima at the Γ point and along the Γ -Z line are located more than 75 meV higher in energy.

The nature (direct/indirect) and magnitude of the gap have been studied experimentally. Transmission measurements of the optical-absorption edge²⁸ indicate the existence of an indirect gap with a magnitude of 0.16 eV. Reflectivity measurements²⁹ predict an indirect gap at 0.150 ± 0.020 eV and a direct one at 0.220 ± 0.020 eV. Our results predict two distinct valence-band maxima that are very close in energy and therefore indicate the existence of both a direct and an indirect band gap of very similar magnitude. The energy difference between the two valence-band maxima is very small (1 meV), smaller than the convergence and interpolation accuracy (10 meV), and cannot be resolved with existing methods. Moreover, additional effects become important at such small energy differences, such as the band-gap renormalization due to electron-phonon coupling and finite carrier occupations, as well as excitonic effects that need to be taken into account when comparing with optical data.

The energy bands near an extremum for an arbitrary \mathbf{k} point in the mirror (yz) plane obey the equation

$$2m_e E_n(\mathbf{k})/\hbar^2 = \alpha_{xx}k_x^2 + \alpha_{yy}k_y^2 + \alpha_{zz}k_z^2 + 2\alpha_{yz}k_yk_z. \quad (1)$$

By fitting the above equation to the calculated energy eigenvalues near the band extrema, we can obtain the effective-mass tensors. Equation (1) has the shape of an ellipse in the mirror plane, whose principal axis is at an angle θ to the y axis, where

$$\tan 2\theta = \frac{2\alpha_{yz}}{\alpha_{zz} - \alpha_{yy}}. \quad (2)$$

The values for the hole and electron effective-mass tensors are listed in Tables II and III, respectively. The two tables show a comparison of our calculated results with experimental values and previous theoretical work. The GW-calculated effective-mass tensor at VBM2 is in better agreement with experiment than that at VBM1, indicating that VBM2 may actually be the absolute valence-band maximum and that Bi₂Te₃ has an indirect minimum energy gap. In general, as also observed in previous calculations, the out-of-plane component (α_{xz}) of the effective-mass tensor is in closer agreement with experiment than the in-plane ones, in part because the bands are strongly nonparabolic and the calculation of the in-plane components involves taking differences between the less significant digits of the energy eigenvalues that carry more numerical noise. Moreover, since the band gap of Bi₂Te₃ is so small, band-gap renormalization effects mentioned above may be important and affect the values of the effective-mass tensor.

IV. CONCLUSION

We calculated the quasiparticle band structure of bismuth telluride within the GW approximation. We found two nearby valence-band extrema in the mirror plane of the Brillouin zone indicating that the material has both a direct and an indirect band gap that lie very close in energy with a value (0.17 eV) that is in very good agreement with experiment. Results for the effective-mass tensor near the valence- and conduction-band extrema are in reasonable agreement with experiment but some discrepancies remain. These may be due to higher order effects that are relatively more important in Bi₂Te₃ due to the small value of the band gap. Our results may assist the understanding of the recently discovered topological insulators and the design of technologically important thermoelectric materials.

ACKNOWLEDGMENTS

We thank Peihong Zhang, Jonathan Yates, Ivo Souza, Feliciano Giustino, and Manish Jain for helpful discussions. This work was supported by National Science Foundation under Grant No. DMR07-05941 and by the Director, Office of Science, Office of Basic Energy Sciences, Division of Materials Sciences and Engineering Division, U.S. Department of Energy under Contract No. DE-AC02-05CH11231. E.K. was supported by DOE and the ‘‘Alexander S. Onassis’’ Foundation. M.L.T. was supported by NSF. Graphics were generated using the XCRYSDEN program (Ref. 31) and the Wannier functions were calculated with the WANNIER90 code (Ref. 21). Computational resources were provided by the Department of Energy at the National Energy Research Scientific Computing Center (NERSC) and Teragrid.

-
- ¹T. M. Tritt, *Science* **283**, 804 (1999).
²A. Majumdar, *Science* **303**, 777 (2004).
³H. Zhang, C.-X. Liu, X.-L. Qi, X. Dai, Z. Fang, and S.-C. Zhang, *Nat. Phys.* **5**, 438 (2009).
⁴Y. L. Chen, J. G. Analytis, J.-H. Chu, Z. K. Liu, S.-K. Mo, X. L. Qi, H. J. Zhang, D. H. Lu, X. Dai, Z. Fang, S. C. Zhang, I. R. Fisher, Z. Hussain, and Z.-X. Shen, *Science* **325**, 178 (2009).
⁵P. Hohenberg and W. Kohn, *Phys. Rev.* **136**, B864 (1964).
⁶W. Kohn and L. J. Sham, *Phys. Rev.* **140**, A1133 (1965).
⁷L. Hedin and S. Lundqvist, *Solid State Physics* **23**, 1 (1970).
⁸M. S. Hybertsen and S. G. Louie, *Phys. Rev. B* **34**, 5390 (1986).
⁹S. G. Louie, in *Conceptual Foundations of Materials: A Standard Model for Ground- and Excited-State Properties*, edited by S. G. Louie and M. L. Cohen (Elsevier, Amsterdam, 2006), p. 9.
¹⁰W. G. Aulbur, L. Jönsson, and J. W. Wilkins, *Solid State Physics* **54**, 1 (1999).
¹¹M. Kim, A. J. Freeman, and C. B. Geller, *Phys. Rev. B* **72**, 035205 (2005).
¹²G. Wang and T. Cagin, *Phys. Rev. B* **76**, 075201 (2007).
¹³S. J. Youn and A. J. Freeman, *Phys. Rev. B* **63**, 085112 (2001).
¹⁴P. Larson, S. D. Mahanti, and M. G. Kanatzidis, *Phys. Rev. B* **61**, 8162 (2000).
¹⁵S. K. Mishra, S. Satpathy, and O. Jepsen, *J. Phys.: Condens. Matter* **9**, 461 (1997).
¹⁶H. Köhler, *Phys. Status Solidi B* **74**, 591 (1976).
¹⁷H. Köhler, *Phys. Status Solidi B* **73**, 95 (1976).
¹⁸M. S. Hybertsen and S. G. Louie, *Phys. Rev. B* **34**, 2920 (1986).
¹⁹N. Marzari and D. Vanderbilt, *Phys. Rev. B* **56**, 12847 (1997).
²⁰I. Souza, N. Marzari, and D. Vanderbilt, *Phys. Rev. B* **65**, 035109 (2001).
²¹A. A. Mostofi, J. R. Yates, Y.-S. Lee, I. Souza, D. Vanderbilt, and N. Marzari, *Comput. Phys. Commun.* **178**, 685 (2008).
²²J. Ihm, A. Zunger, and M. L. Cohen, *J. Phys. C* **12**, 4409 (1979).
²³N. Troullier and J. L. Martins, *Phys. Rev. B* **43**, 1993 (1991).
²⁴S. G. Louie, S. Froyen, and M. L. Cohen, *Phys. Rev. B* **26**, 1738 (1982).
²⁵S. Nakajima, *J. Phys. Chem. Solids* **24**, 479 (1963).
²⁶H. J. Monkhorst and J. D. Pack, *Phys. Rev. B* **13**, 5188 (1976).
²⁷S. Lee and P. von Allmen, *Appl. Phys. Lett.* **88**, 022107 (2006).
²⁸I. G. Austin, *Proc. Phys. Soc. London* **72**, 545 (1958).
²⁹G. A. Thomas, D. H. Rapkine, R. B. Van Dover, L. F. Mattheiss, W. A. Sunder, L. F. Schneemeyer, and J. V. Waszczak, *Phys. Rev. B* **46**, 1553 (1992).
³⁰C.-Y. Li, A. L. Ruoff, and C. W. Spencer, *J. Appl. Phys.* **32**, 1733 (1961).
³¹A. Kokalj, *Comput. Mater. Sci.* **28**, 155 (2003).